

Polyurethane–epoxy based azopolymers: Influence of chemical structure over photoinduced birefringence

Luciana M. Sáiz, Patricia A. Oyanguren, María J. Galante*

Institute of Materials Science and Technology (INTEMA), University of Mar del Plata and National Research Council (CONICET), J.B. Justo 4302, 7600 Mar del Plata, Argentina

ARTICLE INFO

Article history:

Received 20 September 2011

Received in revised form 29 March 2012

Accepted 23 April 2012

Available online 1 May 2012

Keywords:

Polyurethane

Azopolymer

Epoxy

Optical birefringence

ABSTRACT

A comparative study of the influence of the competitive reactions that can take place in epoxy–isocyanate based azo systems over optical behavior was developed.

Diverse disperse red 19 (DR 19) azo urethane oligomers (PUs) were synthesized and characterized using size exclusion chromatography (SEC), Fourier transform infrared (FTIR), and UV–visible spectroscopy. Based on these urethane oligomers, epoxy–PU networks having isocyanurate and oxazolidone rings in their structures were prepared in different isocyanate/epoxy stoichiometric ratios, $r = \text{eq. NCO/eq. epoxy}$ (0.5, 1, and 2).

Photoinduced anisotropy (Δn), remnant birefringence (RB) and dichroism were measured for the resulting polymers and evaluated as function of their T_g s and chemical structures. Final materials exhibited very high values of Δn and RB being promised materials for using in optical storage information devices.

© 2012 Elsevier Ltd. All rights reserved.

1. Introduction

Azopolymers have more stable thermal and mechanical properties than their respective monomers. They have been used to produce optical, artificial taste, and pH sensors. However their main characteristic is the capacity of displaying reversible cis–trans isomerization with very useful applications in optical information storage, light switching devices, surface relief gratings, holograms, and induction of liquid-crystals alignment [1–3].

Recent studies on photo-orientation processes in amorphous polymers have addressed the role of T_g and polymer structural effects, including the main chain rigidity, the nature of the connection of the chromophore to a rigid, semirigid or flexible main chain, the free volume, the free volume distribution or combination of these, over the photo-induced anisotropy [4]. A seemingly small difference in the polymer backbone, for example the presence of an aromatic ring, clearly influences the photoorientation efficiency, confirming the influence of the polymer structure on photoorientation. The observed anisotropy depends on the cis and trans balance in concentration and on the extinction coefficient of the isomers, as well as on their orientation. However, polymers with the same chromophore but different backbones exhibit different levels of induced anisotropy under the same irradiation conditions. It has been observed that the spontaneous, thermally activated relaxation of the chromophores is primarily governed

by the movement of the polymer backbone and not by the movement of the chromophore. Relaxation processes are, in principle, easy to analyze because effects from heating and isomerization rates are small once the laser pump is switched off. So, the three remaining main factors are: the free volume around the azo moiety, the rigidity of the polymer, where longer relaxation times are expected for materials with higher T_g , and cooperative effects that may cause relaxation times to be longer when the amount of chromophore is increased. The residual signal is apparently related to the maximum birefringence but this happens because the latter also depends on the polymer rigidity. The higher the polymer T_g , the lower the maximum induced birefringence was. Also, the time required to achieve 50% of maximum induced birefringence, which can be correlated to the polymer rigidity, is longer for polymers with higher T_g values. Mendonça et al [5] have observed an odd behavior of a DR19–IPDI polyurethane polymer whose maximum birefringence was lower than for DR19–MDI polyurethane, in spite of possessing a slightly larger chromophore concentration. They attributed it to an increase in the degree of electron delocalization in MDI caused by introduction of phenyl rings instead of isophorones groups into the polymer.

Considering the polymer chemical structure when epoxy/isocyanate based materials are studied, it is well known that in the curing of epoxies by isocyanates the reaction between oxirane cycles and isocyanate groups is of great importance; in addition to urethane formation due to the interaction between the secondary hydroxyl group of epoxy oligomers and isocyanate groups. It has been found that, in the presence of catalyst in a

* Corresponding author. Tel.: +54 223 4816600; fax: +54 223 4810046.

E-mail address: galant@fi.mdp.edu.ar (M.J. Galante).

monomeric epoxy–isocyanate mixture, the reaction of oxazolidone formation might be supplemented by trimerization of isocyanate groups, resulting in the emergence of isocyanurate cycles [6].

For epoxy/isocyanate based polymers the amount of catalyst and the stoichiometric ratio between the diisocyanate and the diepoxide, have influence over the glass-transition temperature of the obtained network. A high r (NCO/epoxy) leads to an increase in the cross-linking density because of a greater amount of formed isocyanurate rings. If there are many oxazolidone divalent rings, the cross-linking density is lowered and the mobility of the network is increased [7]. Oxazolidone repeat units have been built into polymers containing isocyanurate crosslinks. The oxazolidone ring has good thermal stability, and also mechanical properties of polymers with this structure have been found to be improved [8].

The difficulty in controlling the synthesis of this kind of polymers in order to obtain materials with the best properties combination deals, in consequence, with the competition among the diverse reactions that could take place in an epoxy/isocyanate blend. The relative proportion of different groups will depend on factors such as: structure and concentration of monomers, type and concentration of catalyst and cycles of curing and postcuring.

To elucidate the influence of some of these factors over optical properties, different epoxy/isocyanate based azopolymers were

synthesized, characterized and their properties evaluated and compared in terms of birefringence and dichroism. Also, the effect of temperature over the induced birefringence was evaluated.

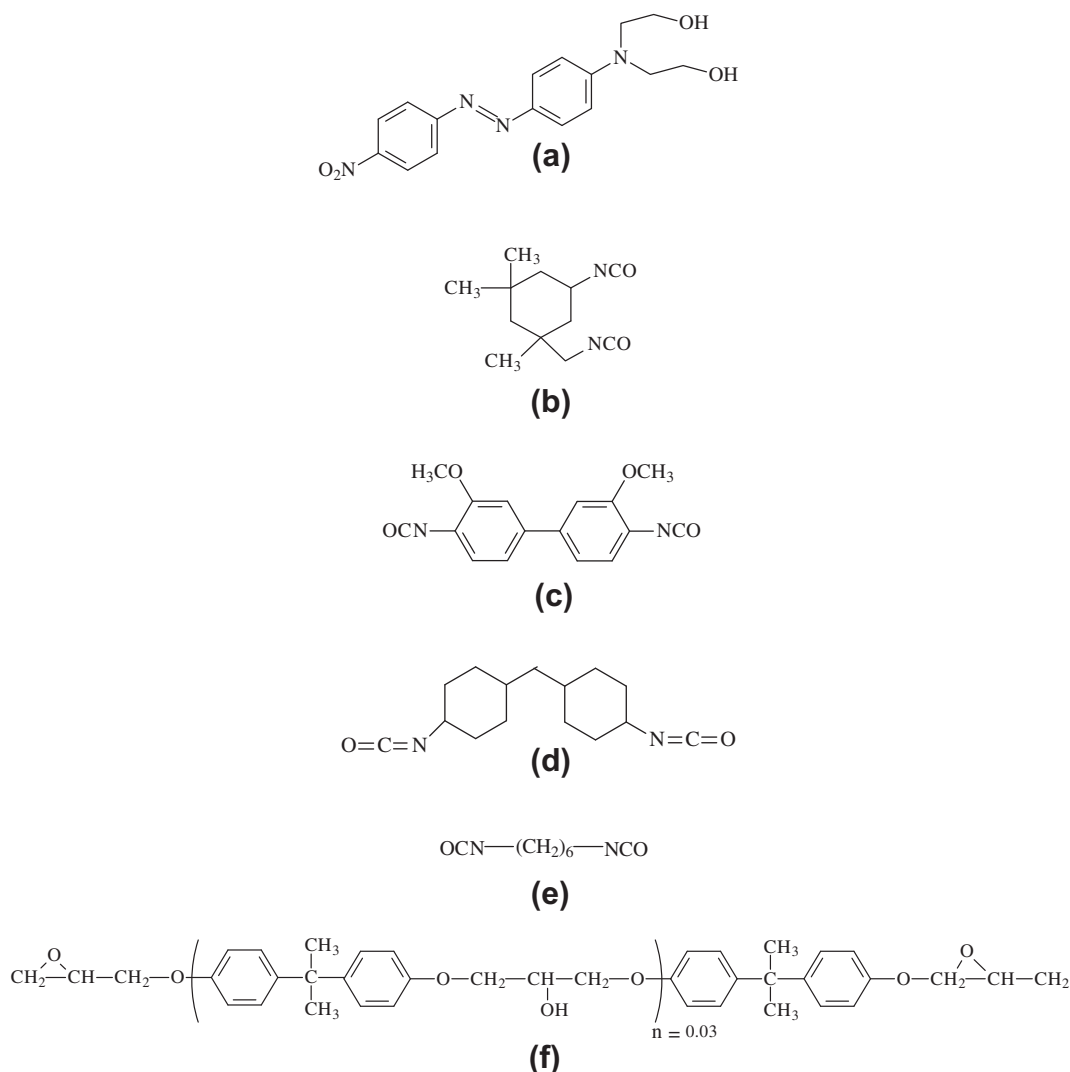
2. Experimental section

2.1. Materials

A push–pull azo chromophore was selected as photosensitive reactive. It was $C_6H_3(NO_2)N=NC_6H_4N(CH_2CH_2OH)_2$ (Disperse Red 19, DR19, Aldrich), with a $T_m = 300$ °C and a dye content of 95%. Isophorone diisocyanate (D1, Aldrich, 98%), 3,3'-dimethoxy-4,4'-diphenylenediisocyanate (D2, Aldrich, 90%), 4,4'-metylenbis(cyclohexylisocyanate) (D3, Aldrich, 85%) and 1,6-diisocyanatehexane (D4, Aldrich, 99%) were employed in the synthesis of azo-urethane oligomers. Dibutyltin dilaurate (DBTDL, Aldrich) was used as a catalyst for the synthesis.

Reactions were carried out in tetrahydrofuran (THF, Biopack, 99%) or *N,N*-dimethylformamide (DMF, Anedra, 99,9%) that were distilled from calcium chloride and stored over 3 Å molecular sieves.

The diepoxide was based on diglycidyl ether of bisphenol A (DGEBA, Der 332, Fluka) with a mass per mol of epoxy groups



equal to 174 g mol^{-1} . Benzyltrimethylammonium (BDMA, Aldrich) was used as a catalyst for the epoxy–isocyanate reaction. Chemical structures of the different reactants are shown in Fig. 1.

2.2. Synthesis of azo oligomers

The oligomers were prepared according to the reaction scheme shown in Fig. 2.

2.2.1. Oligomer PU1

Disperse Red 19 (0.165 g, 0.5 mmol) and isophorone diisocyanate (D1) (0.222 g, 1 mmol) were dissolved in about 20 ml of distilled THF. DBTDL (1.6 g of DBTDL/100 g of D1) was added as a catalyst. The resulting mixture was heated at 55°C for 2 h and then was cooled to room temperature.

2.2.2. Oligomer PU2

Disperse Red 19 (0.165 g, 0.5 mmol) and 3,3'-dimethoxy-4,4'-diphenylene diisocyanate (D2) (0.296 g, 1 mmol) were dissolved in about 20 ml of distilled DMF. DBTDL (1.6 g of DBTDL/100 g of D2) was added as a catalyst. The resulting mixture was heated at 70°C for 2 h and then was cooled to room temperature.

2.2.3. Oligomer PU3

Disperse Red 19 (0.165 g, 0.5 mmol) and 4,4'-methylene-bis(cyclohexyl isocyanate) (D3) (0.262 g, 1 mmol) were dissolved in about

20 ml of distilled THF. DBTDL (1.6 g of DBTDL/100 g of D1) was added as a catalyst. The resulting mixture was heated at 55°C for 1 day and then was cooled to room temperature.

2.2.4. Oligomer PU4

Disperse Red 19 (0.165 g, 0.5 mmol) and 1,6-diisocyanatehexane (D4) (0.168 g, 1 mmol) were dissolved in about 20 ml of distilled THF. DBTDL (1.6 g of DBTDL/100 g of D4) was added as a catalyst. The resulting mixture was heated at 55°C for 2 h and then was cooled to room temperature.

2.3. Synthesis of azo networks and films preparation

The solution of PU and DGEBA was mixed using different stoichiometric ratios, $r = \text{eq. NCO}/\text{eq. epoxy}$ ($r = I/E$) comprised between 0.5 (epoxy excess) and 2 (isocyanate excess), using 1% BDMA (mole per isocyanate equivalent) to initiate the reaction. Films were prepared by spin-coating using a single wafer spin processor (Model WS-400E-6NPP-lite, by Laurell) from the reactive mixture solutions onto glass slides previously cleaned using the standard RCA method [9], and NaCl windows. The spinner cycle program was as follows: 1000 rpm for 30 s, 4000 rpm for 10 s, and 8000 rpm for 20 s. The films were cured at 100°C for 1 h, 180°C for 1 h, and 1 h 200°C in a vacuum oven. After curing, films were heated above their glass transition temperatures, in order to erase any preferential orientation of the chromophores during films preparation. Samples were subsequently stored at room temperature.

2.4. Measurements

Size exclusion chromatography was used to follow PU reaction and to determine the molar mass distribution of oligomers obtained. A Knauer chromatograph (SEC) equipped with a separate sample injection camera, HPLC pump (K-501, Knauer), two columns packed with styrene-divinylbenzene $5 \mu\text{m}$ copolymer particles (Phenomenex Phenogel 50, Waters Styragel HR1, – nominal pore sizes of 50 \AA , 100 \AA), and a refractive index detector (RI detector K-2301 Knauer) was used. The mobile phase was THF with an elution rate of 0.35 mL/min . Molecular weights were referred to a polystyrene calibration using polystyrene standards. All the scans were performed at room temperature.

A FT-IR Nicolet 6700 Thermo Scientific device was employed to obtain IR spectra in the mid-IR range ($400\text{--}4000 \text{ cm}^{-1}$). Differential scanning calorimetry (DSC) was performed using a Pyris 1 Perkin – Elmer device. Glass transition temperature (T_g) of the polymers was determined from the thermograms as the onset of the change in specific heat in heating scans at 10°C/min .

UV–visible spectra of DR19 and the azo oligomers (PUs) in THF or DMF solutions were recorded on an Agilent 8453 UV–visible spectrophotometer.

Photoorientation experiments were carried out at room temperature and under ambient conditions, each time on a different non previously irradiated spot, to avoid irradiation history influences. The optical configuration for the measurement of photoinduced birefringence was similar to that previously reported [10]. Photoinduced birefringence of the resulting films was measured by placing the sample between two crossed linear polarizers. A semiconductor laser at 488 nm was used as writing beam to induce optical anisotropy in the polymeric film, and a semiconductor laser at 635 nm was used as reading beam to measure the power that is transmitted through this optical setup. To achieve maximum signal, the polarization vector of the writing beam was set to 45° with respect to the polarization vector of the reading beam. All the films were irradiated with 6 mW/mm^2 of the writing laser in a 0.785 mm^2 spot.

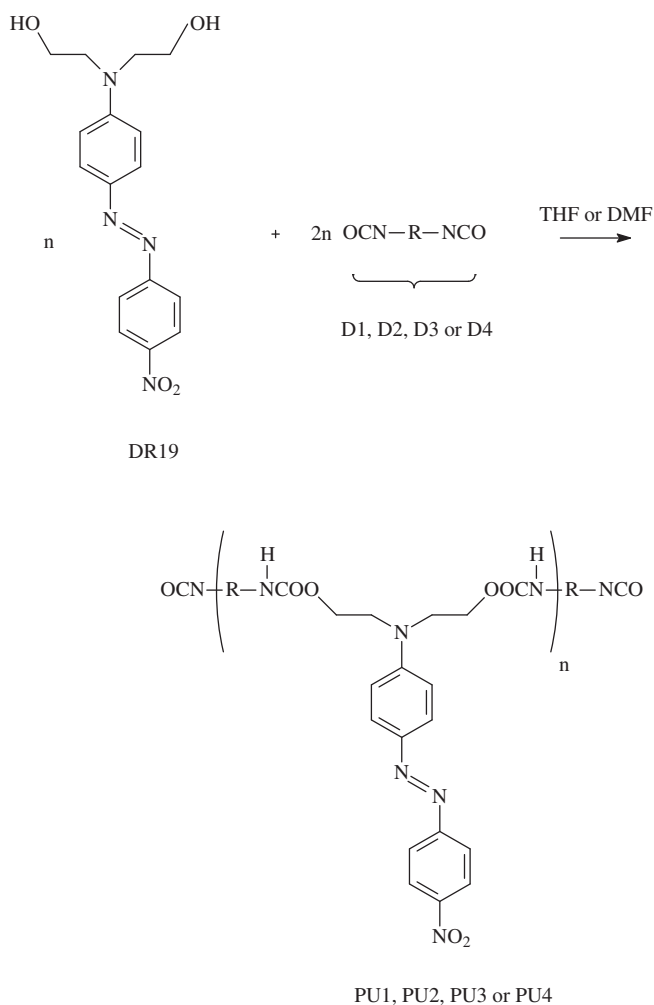


Fig. 2. Synthesis schemes for the oligomers PU1, PU2, PU3 and PU4.

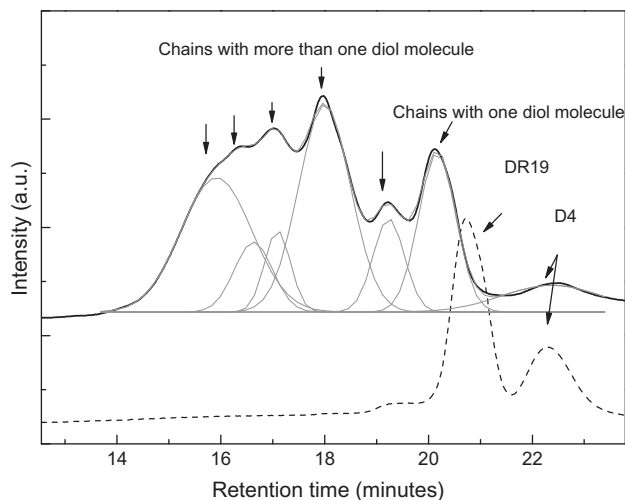


Fig. 3. SEC chromatogram of reaction products, compared with SEC chromatograms of monomers (DR19 and D4).

Measurements at elevated temperature were made setting the sample in a hot stage Linkman THMS 600.

The induced birefringence was determined by measuring the probe beam transmission ($T = I/I_0$) according to:

$$\Delta n = (\lambda/\pi d) \sin^{-1}(I/I_0)^{1/2} \quad (1)$$

where λ is the wavelength of the writing beam, d is the film thickness, I is the intensity after the second polarizer, and I_0 is the transmitted intensity between parallel polarizers, in absence of anisotropy.

The films thicknesses were obtained from topographic images obtained by Atomic Force Microscopy (AFM, 5500 SPM Agilent Technologies) in contact mode.

Dichroism measurements were made from UV–visible spectra recorded with the Agilent 8453 UV–visible spectrophotometer, fitted with polarizing optics. The films were exposed to a linearly polarized semiconductor laser beam at 488 nm for time enough to reach saturation, and UV–visible spectra of films, for light polarized parallel and perpendicular to the writing polarization direction were recorded on the relaxed films. The dichroism ratio of the films, D , was calculated from the measured absorbance at maximum wavelength (λ_{\max}) perpendicular (A_{\perp}) and parallel (A_{\parallel}) to the electric vector of the incident light.

$$D = A_{\perp}/A_{\parallel} \quad (2)$$

3. Results and discussion

3.1. Characterization of the oligomers

Azo urethane oligomers (PUs) were synthesized by reaction between DR19 and diisocyanates D1, D2, D3 or D4 (DI). The samples were prepared in a stoichiometric ratio $r = \text{eq. DR19}/\text{eq. DI} = 0.5$, to generate reaction products with isocyanate groups in the extreme of chains. Monomers were mixed at room temperature and reactions were performed inside closed tubes in an oil bath.

The products distribution during reaction was followed by SEC. As an example, Fig. 3 shows SEC chromatograms of the reagents, DR19 and D4, and the oligomers PU4. Chromatograms of the reagents show an intensive peak at 20 min assigned to azo diol, DR19, and a peak located at 22.3 min, corresponding to diisocyanate D4.

The SEC chromatograms of PUs show a broad distribution of products generated by the diol–diisocyanate reaction. Three

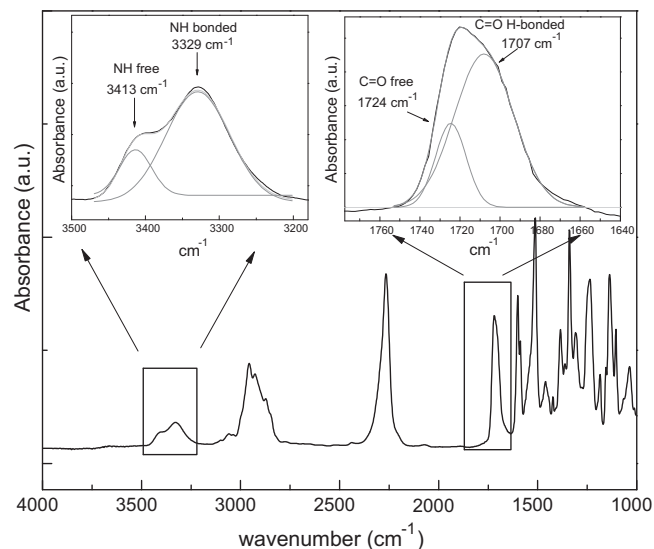


Fig. 4. FTIR spectrum of PU1.

different species could be identified in the synthesis of linear polyurethanes with terminal isocyanate groups: free diisocyanate, chains with a molecule of diol, and chains with more than a molecule of diol in their structure. FTIR spectra of the polyurethane samples in the mid-IR region were also obtained. As an example, Fig. 4 shows the FTIR spectrum of PU1. The peaks at 1515 cm^{-1} and 1335 cm^{-1} were attributed to the asymmetric and symmetric vibrations of $-\text{NO}_2$ groups respectively, and the band at 1404 cm^{-1} to the tension vibration of the $\text{N}=\text{N}$ linkage of the azo chromophore. It is well recognized that the band of the $\text{N}-\text{H}$ stretching mode is composed of two main contributions, attributed to “free” (non-hydrogen bonded) and hydrogen bonded to $\text{N}-\text{H}$ groups. Examination of the $\text{N}-\text{H}$ stretching region of the infrared spectra of the oligomers recorded at room temperature leads one to conclude that the band envelope is composed of at least two contributing bands. Curve fitting in the $\text{N}-\text{H}$ stretching region was performed on the spectra. A linear base line was drawn from 3600 cm^{-1} to 2900 cm^{-1} . The limit of the curve-fitting procedure was set between 3500 cm^{-1} and 3200 cm^{-1} . Two Gaussian bands, corresponding to the free and hydrogen bonded $\text{N}-\text{H}$ groups, were employed in the curve-fitting procedure. The infrared bands at 3420 cm^{-1} and 3320 cm^{-1} were assigned to the $\text{N}-\text{H}$ stretching modes of the free and hydrogen bonded $\text{N}-\text{H}$ groups of polyurethane.

The carbonyl stretching region of the spectra of PUs also suggests the presence of at least two bands, at about 1700 cm^{-1} and 1720 cm^{-1} , depending on the diisocyanate employed. These bands could be attributed to hydrogen bonded carbonyl groups and “free” carbonyl groups, respectively. Curve fitting in the carbonyl stretching region was performed in a similar manner to that previously described for the $\text{N}-\text{H}$ stretching region. A linear base line was drawn between 1500 cm^{-1} and 2000 cm^{-1} . The limit of the curve-fitting procedure was set between 1675 cm^{-1} and 1780 cm^{-1} . Two Gaussian bands, corresponding to “free” and hydrogen bonded were employed in the curve-fitting procedure. A representative example of the spectral components obtained from curve-fitting procedure for PU1 is shown in Fig. 4.

3.2. FTIR analysis of the polymer networks

Reaction between a diepoxide and a diisocyanate leads to polymer networks characterized by the presence of isocyanurate and oxazolidone rings in their chemical structure. Main reactions taking place in an epoxy–isocyanate–tertiary amine system are

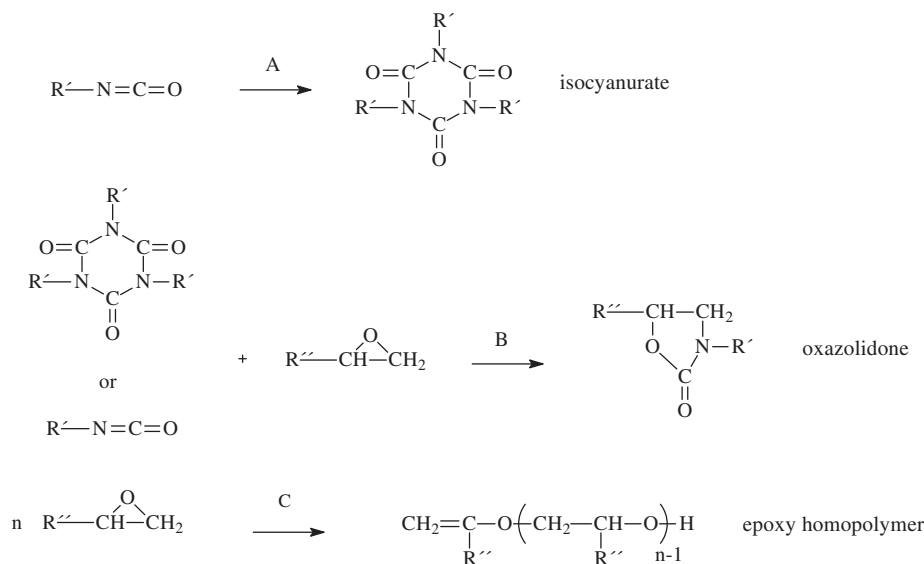


Fig. 5. Main reactions taking place in an epoxy/isocyanate/tertiary amine system.

described in Fig. 5. The fraction of the different components present in the final network depends on the initial isocyanate/epoxy ratio, I/E , the diisocyanate employed, the type of catalyst and the cure cycle [7].

To analyze the reactions in the present systems, FTIR spectra were recorded for PU oligomers, reacting with DGEBA at different temperatures, for different periods of time. Fig. 6 shows the spectra of PU1-DGEBA prepared in $r = 1$. When the oligomer was mixed with a stoichiometric amount of diepoxy and heated, the peak at 2260 cm^{-1} associated with the free isocyanate in the oligomers and the peak at 910 cm^{-1} associated with the epoxy group decreased, while the polyurethane peak in the carbonyl region increased in height and width. The evolution of the different groups in the NH stretching and the carbonyl regions is shown in Fig. 7 and 8. Curve fitting in the N–H stretching and carbonyl stretching regions was performed in the manner that was previously described. We established that the first reaction was

the formation of isocyanurate rings, characterized by a peak at about 1710 cm^{-1} . At high temperatures, the formation of oxazolidone rings, characterized by a peak at about 1760 cm^{-1} , took place by reaction between isocyanate and epoxy groups. The decomposition of isocyanurate ring in the presence of an epoxy excess also gives oxazolidone rings. The appearance of OH groups (characterized by a peak at 3500 cm^{-1}) may be attributed to some epoxy homopolymerization taking place in this temperature range, in which OH groups are generated in the course of a transfer step during anionic polymerization [11,12].

Tables 1 and 2 show how the IR absorption bands change with r . It can be seen that decreasing the I/E ratio, the intensity of absorption due to isocyanurate groups became smaller, while that the band corresponding to oxazolidone groups grew. This means that an isocyanate excess favors reaction occurring at low temperature, it is the isocyanurate formation, meanwhile an epoxy excess promotes reaction taking place at high temperature, the oxazolidone development. In consequence, the increase in $r = I/E$ ratio in the initial formulation leads to an increase in the fraction of isocyanurate

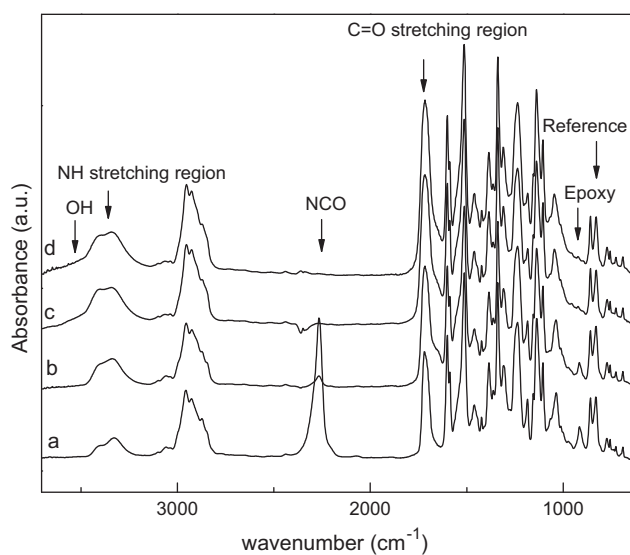


Fig. 6. FTIR spectra of PU1-DGEBA samples ($r = 1$), reacted during different periods of time at different temperatures: (a) 25 °C, (b) 1 h 100 °C, (c) 1 h 100 °C, 1 h 180 °C, (d) 1 h 100 °C, 1 h 180 °C, 1 h 200 °C.

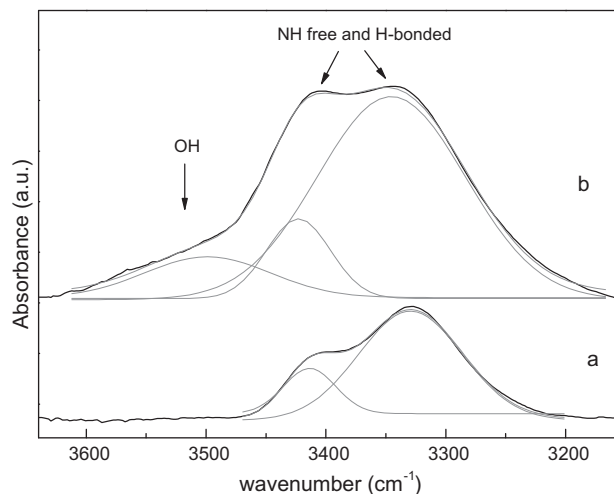


Fig. 7. Curve-fitting results in the N–H stretching region of PU1-DGEBA ($r = 1$) spectrum recorded (a) before and (b) after curing.

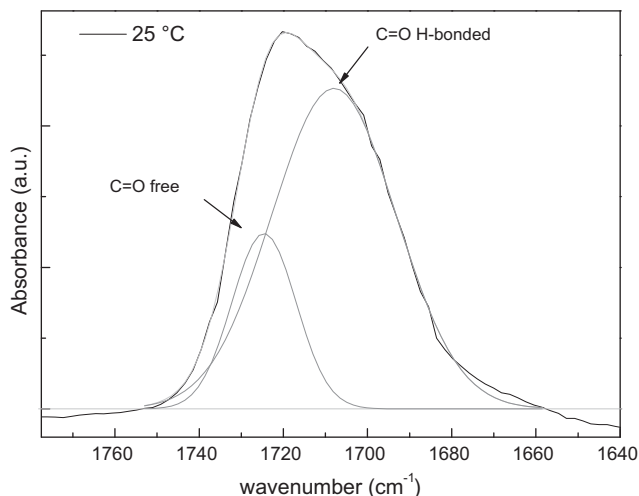


Fig. 8. Curve-fitting results in the carbonyl stretching region of the PU1-DGEBA spectrum recorded during the reaction at 25 °C.

Table 1

Isocyanurate (Iso, $1710 \pm 10 \text{ cm}^{-1}$) and oxazolidone (Oxa, $1760 \pm 10 \text{ cm}^{-1}$) fractions of the total carbonyl area of the FTIR spectrum.

Sample	PU1-DGEBA		PU2-DGEBA		PU3-DGEBA		PU4-DGEBA	
	Iso	Oxa	Iso	Oxa	Iso	Oxa	Iso	Oxa
$r = 0.5$	0.16	0.28	0.02	0.12	0.29	0.19	0.10	0.038
$r = 1$	0.26	0.14	0.19	0.05	0.32	0.02	0.082	0.10
$r = 2$	0.41	0.06	0.54	0.01	0.38	0.002	0.56	0.136

Table 2

Epoxy homopolymerization fraction (3500 cm^{-1}) of the FTIR spectrum.

Sample	PU1-DGEBA	PU2-DGEBA	PU3-DGEBA	PU4-DGEBA
$r = 0.5$	0.32	0.10	0.18	0.29
$r = 1$	0.13	0.05	0.09	0.051
$r = 2$	0.06	0.052	0	0.088

Table 3

Glass transition temperature for the diverse PU-DGEBA polymers prepared in different $r = I/E$.

Sample	PU1-DGEBA	PU2-DGEBA	PU3-DGEBA	PU4-DGEBA
$r = 0.5$	121	141	120	94
$r = 1$	125	155	130	100
$r = 2$	130	163	140	105

over oxazolidone rings and in the corresponding glass transition temperature of the resulting networks [7] (Table 3).

3.3. Optical behavior of the azo-networks

In this section, we will discuss in what extent the structure of the polymer to which the azobenzene is anchored can influence

Table 4

Optical storage properties of the films.

Sample	PU1-DGEBA			PU2-DGEBA			PU3-DGEBA			PU4-DGEBA		
	$r = 0.5$	$r = 1$	$r = 2$	$r = 0.5$	$r = 1$	$r = 2$	$r = 0.5$	$r = 1$	$r = 2$	$r = 0.5$	$r = 1$	$r = 2$
DR19%	22.41	29.38	34.74	19.14	24	27.48	21.26	27.43	32.08	24.19	32.51	39.26
RB%	68	66	65	79	81	82	70	72	69	59	61	63
Δn	0.034	0.043	0.065	0.065	0.077	0.092	0.043	0.043	0.041	0.049	0.054	0.075
D	–	1.17	–	–	1.40	–	–	1.33	–	–	1.18	–

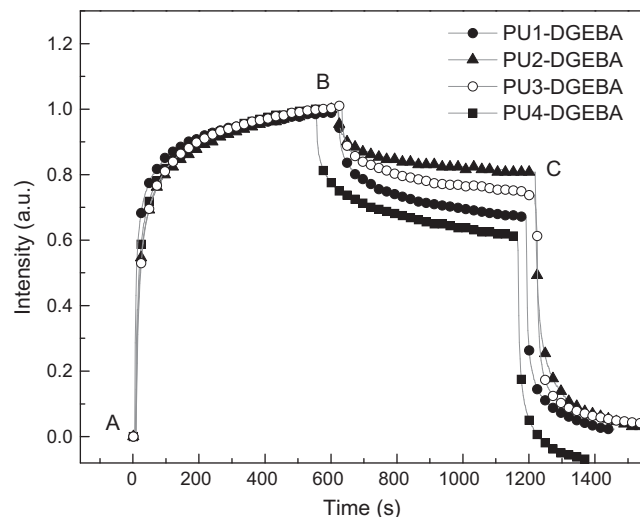


Fig. 9. Typical writing, relaxing and erasing sequences of the different PU-DGEBA films prepared in $r = I/E = 1$.

the chromophore photoorientation. For the different azo-networks obtained, each with distinct characteristics in the molecular structure of the unit building blocks, based in the different structures of the employed isocyanates; birefringence and dichroism were measured and compared for networks prepared in different $r = I/E$ stoichiometric ratios.

A typical sequence of events is presented in Fig. 9 for PU-DGEBA films ($r = 1$). From the resulting curves, it can be seen, that different PU-DGEBA exhibited similar writing slopes, which is traduced in similar writing rates. It was an expected result in virtue of that the rate of achieving birefringence depends principally on the type of the azo group present in the material [13], being DR19 for our polymers. Evaluating chemical structure of the networks, PU2-DGEBA, with two aromatic rigid rings in the isocyanate structure, and with a high degree of electrons delocalization have an optimum optical behavior, i.e. maximum anisotropy ($\Delta n = 0.077$) and remnant birefringence (RB = 81%) (Table 4).

Moreover, the level of maximum birefringence achieved and RB are very high for all PU-DGEBA networks, considering that its wt.% of DR19 is around 30 wt.%. Rochon et al. [14–16], have been demonstrated that for a series of azo-modified polymers the maximum variation in refractive index obtained was 0.08. As well, if we compared our results with previously reported systems [5], we observed similar Δn values for Langmuir-Blodgett films of DR19 based polyurethanes, but with much higher chromophore concentrations (64 wt.%).

If remnant birefringence is evaluated as function of T_g value (Fig. 10), % of RB increases with T_g of PU-DGEBA. Taking into account the T_g value of each PU-DGEBA (Table 3), an easier mobility of the azo-chromophore in the samples with low T_g is expected, due to the rotational motion of trans isomers is considered to be restricted into a small free volume and the glass transition temperature can be a guide to predict the relative size of the free volumes [17]. However, meanwhile in the case of different of PU-DGEBA

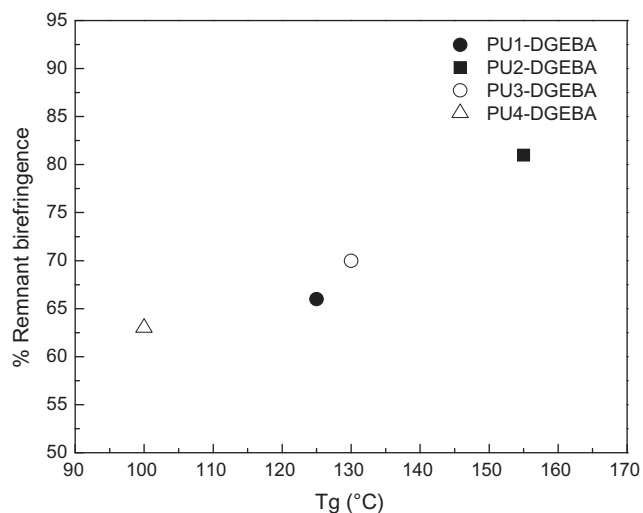
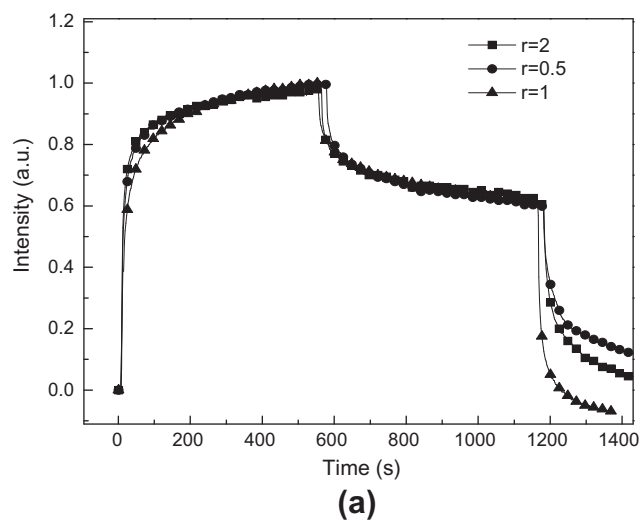
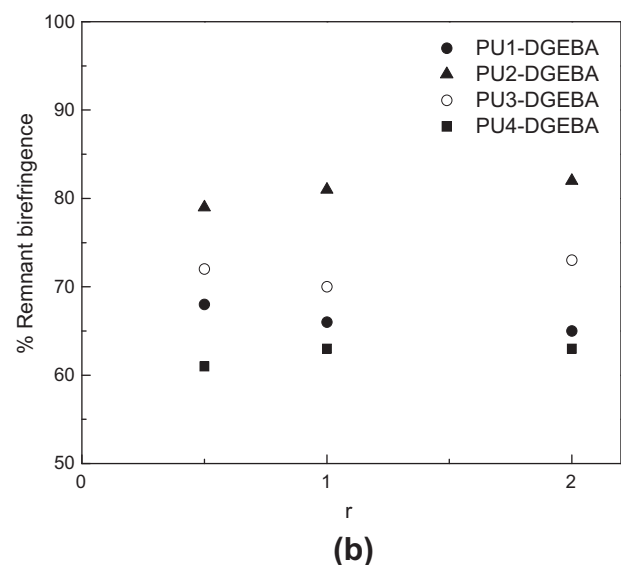


Fig. 10. Remnant birefringence vs. glass transition temperature for the different PU-DGEBA ($r = 1$).



(a)



(b)

prepared in similar stoichiometric ratio ($r = 1$) we observed that this trend is followed; for films of PU-DGEBA prepared in different $r = I/E$ ($r = 0.5, 1$ and 2), the behavior was different. They exhibited similar values of remnant birefringence, despite the fact of possessing different T_g s or polymer chemical structure (different fraction of isocyanurate or siad oxazolidone rings) (Fig. 11a and b) (Table 3). In this case the spontaneous, thermally activated relaxation of the chromophores seems to be primarily governed by the movement of the diisocyanate directly bonded to the azo chromophore more than the nature of the polymer to which is bonded. When the induced anisotropy is analyzed as a function of the isocyanate structure (Table 4), we can point out that the polymer based on an aromatic isocyanate (PU2-DGEBA) exhibited the maximum anisotropy for the three different $r = I/E$ ($0.5, 1$ and 2). In addition, except in the case of PU3-DGEBA (in which not clear differences were observed) the birefringence increases with r , i.e.: with the increase in concentration of isocyanurate rings with respect to oxazolidone groups. It is important to added that there is also a small increase in azo chromophore wt.% from 19.1 wt.% for $r = 0.5$, to 27.5 wt.% for $r = 2$, which would also contribute to the increase in birefringence.

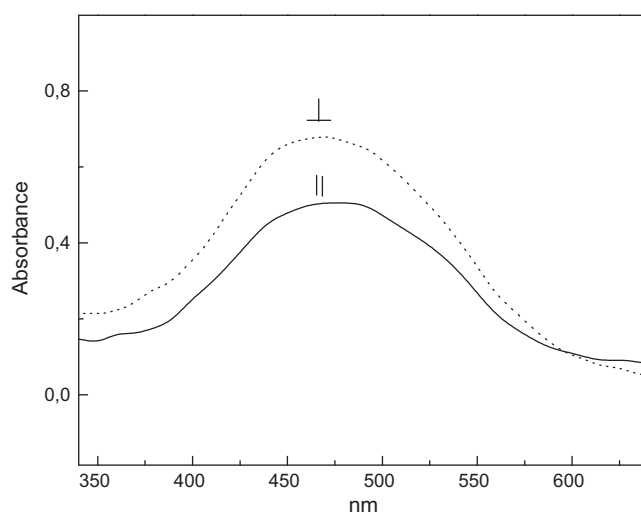


Fig. 12. UV-visible spectra of PU3-DGEBA for light polarized perpendicular and parallel to the writing direction.

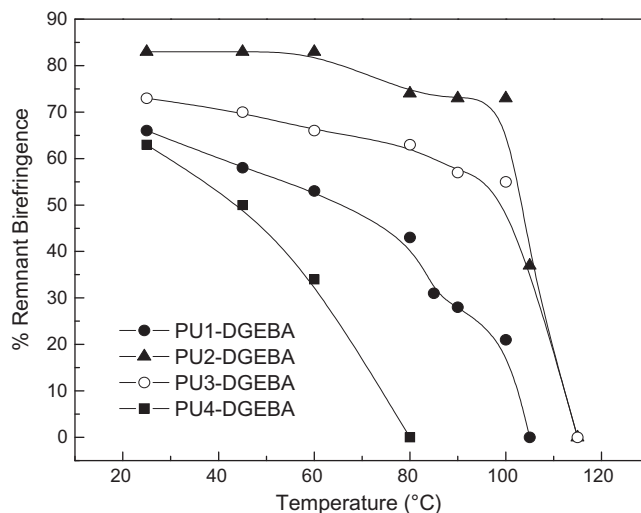


Fig. 13. Remnant birefringence as a function of increasing temperature for the different PU-DGEBA samples with $r = 1$.

Fig. 11. (a) Writing, relaxing, and erasing sequences for PU4-DGEBA films prepared in variable $r = I/E$ ratio; (b) Remnant birefringence vs. $r = I/E$ for the different PU-DGEBA polymers.

Typical examples of the optically induced dichroism are presented in Fig. 12, where the polarized UV–visible absorption spectra of PU–DGEBA films are shown. The dichroism was measured in the relaxed material. It is clear shown that the absorption coefficient for light polarized parallel to the writing direction is substantially lower than that for light polarized in the perpendicular direction. The dichroic ratios for the different PU–DGEBA samples ($r = 1$) are given in Table 4. The obtained dichroism values are directly related to the remaining birefringence. PU2–DGEBA films display higher RB and in concordance, the higher dichroism ($D = 1.40$).

The influence of temperature over the photoinduced birefringence was also evaluated for the different PU–DGEBA ($r = 1$). It is very well known that an increase in temperature affects the two main processes that must be considered in photoinduced anisotropy: photo isomerization and molecular reorientation. On one hand, increasing the temperature leads to a faster interconversion of the two isomers, which is the cause of more molecular reorientation. On the other hand, the mobility of the molecules increases with temperature, which induces more fluctuations. Up to certain temperature, both processes increase birefringence. At higher temperatures, molecular reorientation will decrease due to thermal vibration of the molecules [18]. So, birefringence can be induced even close to T_g , but is not stable due to thermal motion [16,19]. Jin et al [20] have observed that both the maximum birefringence and the remnant anisotropy decrease with increasing temperature, but the degree of decaying is different for diverse polymers. In our case, a similar qualitative behavior with temperature was developed for networks based on the different isocyanates, i.e. the optical properties diminish with the increase in temperature. The % of remnant birefringence decays with temperature at a distinguishable rate for each PU–DGEBA (Fig. 13). The decrease is faster for PU4–DGEBA, the polymer with the lowest T_g . The resulting trend allows us to think that polymers with higher T_g exhibit the better optical stability with temperature.

4. Conclusions

Different PU–DGEBA azopolymers were synthesized and characterized; and their optical properties measured and compared. The obtained materials having isocyanurate and oxazolidone rings, exhibited T_g values which varied as a function of the relative concentration of each one of the rings in their chemical structures.

Concerning the optical behavior of the different polymers, it is interested to point out that the structure, and in consequence the ability to move of the isocyanate directly bonded to the azo group

has determined the storage capability of the polymer, more than its T_g . It was observed when materials based in the same isocyanate but exhibiting different $r = I/E$, and in consequence different T_g , were compared.

When the effect of temperature over optical anisotropy was analyzed, it was observed that the rate at which the remnant birefringence decreased with temperature was a function of the PU T_g .

In summary, playing with the chemical reactants and their stoichiometric ratio, we were able of synthesizing PU–epoxy network with different structure and thermal properties. The final polymers exhibited high values of photoinduced anisotropy and remnant birefringence, resulting promising materials to be used in optical storage devices and others optical applications.

Acknowledgements

We acknowledge the financial support of the National Research Council (CONICET, Argentina), the National Agency for the Promotion of Science and Technology (ANPCyT, Argentina), and the University of Mar del Plata (Argentina).

References

- [1] P. Alessio, D.M. Ferreira, A.J. Job, R.F. Aroca, A. Ruil Jr., C.J.L. Constantino, E.R. Pérez González, *Langmuir* 24 (2008) 4729–4737.
- [2] A. Natansohn, P. Rochon, *Chem. Rev.* 102 (2002) 4139–4176.
- [3] T. Ikeda, *J. Mater. Chem.* 13 (2003) 2037–2057.
- [4] Z. Sekkat, D. Yasumatsu, S. Kawata, *J. Phys. Chem. B* 106 (2002) 12407–12417.
- [5] C.R. Mendonça, D.S. dos Santos Jr., D.T. Balogh, A. Dhanabalan, J.A. Giacometti, S.C. Zilio, O.N. Oliveira Jr., *Polymer* 42 (2001) 6539–6544.
- [6] T.I. Kadurina, V.A. Prokopenko, S.I. Omelchenko, *Polymer* 33 (1992) 3858–3864.
- [7] D. Caille, J.P. Pascault, L. Tighzert, *Polym. Bull.* 24 (1990) 23–30.
- [8] J.S. Senger, I. Yilgor, J.E. Mc Grath, *J. Appl. Polym. Sci.* 38 (1989) 373–382.
- [9] W. Kern, *Semicond. Int.* 7 (1984) 94–99.
- [10] L.M. Sáiz, A.B. Orofino, M.M. Ruzzo, G. Arenas, P.A. Oyanguren, M.J. Galante, *Polym. Int.* 60 (2011) 1053–1059.
- [11] M.J. Galante, A. Vazquez, R.J.J. Williams, *Polym. Bull.* 27 (1991) 9–15.
- [12] A. Vazquez, R. Deza, R.J.J. Williams, *Polym. Bull.* 28 (1992) 459–465.
- [13] M.S. Ho, A. Natansohn, P. Rochon, *Macromolecules* 28 (1995) 6124–6127.
- [14] P. Rochon, J. Gosselin, A. Natansohn, S. Xie, *Appl. Phys. Lett.* 60 (1992) 4–5.
- [15] A. Natansohn, P. Rochon, J. Gosselin, S. Xie, *Macromolecules* 25 (1992) 2268–2273.
- [16] X. Meng, A. Natansohn, P. Rochon, *J. Polym. Sci., Part B: Polym. Phys.* 34 (1996) 1461–1466.
- [17] R. Fernández, I. Mondragon, M.J. Galante, P.A. Oyanguren, *Eur. Polym. J.* 45 (2009) 788–794.
- [18] E. Mohajeranr, N. Nataj, *Opt. Mater.* 29 (2007) 1408–1415.
- [19] D. Hore, A. Natansohn, P. Barret, *Can. J. Chem.* 76 (1998) 1648–1653.
- [20] M. Jin, Q.X. Yang, R. Lu, L.Y. Pan, W.Y. Qi, Y.Y. Zhao, *Mater. Chem. Phys.* 82 (2003) 246–252.